

Dynamic Modeling and Inverse Dynamic Analysis of Flexible Parallel Robots

Du Zhaocai and Yu Yueqing

College of Mechanical Engineering & Applied Electronics Technology , Beijing University of Technology , Beijing, China

Corresponding author E-mail: duzhaocai@emails.bjut.edu.cn

Abstract: This paper presents a method for the dynamic modeling of parallel robots with flexible links and rigid moving platform based on finite element theory. The relation between elastic displacements of links is investigated, taking into consideration the coupling effects of elastic motion and rigid motion. The kinematic and dynamic constraint conditions of elastic displacements of flexible parallel robots are presented. The Kineto-Elastodynamics theory and Timoshenko beam theory are employed to derive the equations of motion, considering the effects of distributed mass, lumped mass, rotary inertia, shearing deformation, bending deformation, lateral deformations and all the dynamic coupling terms. The dynamic behavior due to flexibility of links is well illustrated through numerical simulation. Compared with the results of SAMCEF software simulation, the numerical simulation results show good coherence and the advantages of the method. The flexibility of links is demonstrated to have significant impact on system performance and stability. A method for the inverse dynamic analysis of flexible parallel robots is presented.

Keywords: flexible parallel robot, flexible link, dynamic modeling, inverse dynamic analysis

1. Introduction

The parallel robot has been an advanced topic in robotics research. Parallel robots are widely used in many applications (Lebret, G. et al, 1993), such as entertainment, home services, flying machines, submarines, assembling robots, etc. Planar parallel robots are good candidates for microminiaturization into micro-devices. Compared with serial robots, parallel robots are provided with a series of advantages in terms of heavy payload, small error, high positional accuracy, ease of control, and so on. Currently, many industries generally use serial robots in operations. Results are good, but both accuracy and throughput could be significantly improved by using parallel robots (Gabriel P., 2003).

Several researchers have studied parallel robots, but most of the researches have been restricted to the rigid parallel robot (Liu, K. et al, 1993 ; Liu, K. et al, 1994). Few investigations (Wang, X Y., 2005 ; Wang, X Y. & James, K M., 2006) have been concerned with the flexible parallel robot.

The trend towards higher operating speed and use of less material requires that some phenomena which used to be omitted have to be taken into account in dynamic analysis, and it is necessary to consider links' flexibility and coupling effects of the flexible links' elastic displacement. The dynamics of flexible robots working at high speed has been studied by many researchers (Book, W J., 1990 ; Gaultier, P E. & Cleghorn, W L., 1989 ; Santosha K D. & Peter E. 2006), and a number of

approaches have been developed to predict the elastic dynamic behavior of flexible serial robots. Some researchers have proposed an efficient procedure for computer generation of symbolic modeling equations for planar serial robots with rigid and flexible links (Wang, D. & Vidyasagar, M., 1992 ; Lin, J. & Lewis, F L., 1994). Because of the complexity resulting from the presence of multi-closed loops and the limitation of computer facilities accessible, this method may not be suitable for parallel robots with flexible links and rigid moving platform.

In recent years, parallel robots have received more and more attention. Although several investigators have used finite element techniques to model flexible parallel robots, they did not include all the influences below (Benosman, M. & Le, V G., 2002 ; Fattah, A. et al, 1994):

- (a) Lumped mass, rotary inertia.
- (b) Shearing deformation, bending deformation, lateral deformation.
- (c) All the dynamic coupling terms.

Till now, a practical method to enable designers to predict the elastic dynamic behavior of parallel robots with flexible links and rigid moving platform has not been available. It is believed that a comprehensive dynamic model is crucial in the design process, in performance evaluation and for control purposes.

The Kineto-Elastodynamics (KED) theory studies moving mechanisms, taking into account deformations of the flexible links due to external and internal loads. The elastic deformations of the links play a significant role in

high-speed operations because the links are usually lighter in weight, and the internal forces are greater. The objective of the investigation in this paper is to develop a simple and efficient method for dynamic modeling and inverse dynamic analysis of flexible parallel robots. This is achieved using the KED theory (Fraid, M. & Lukasiewicz, S A., 2000 ; Jerzy, Z. & Plosa, S W., 2000 ; Yang, J. & Sadler, P., 2000 ; Zhang, C. et al., 1997) and considering the elastic displacement of links and dynamic coupling effects. The effects of distributed mass, lumped mass, rotary inertia, shearing deformation, bending deformation and lateral deformation are all taken into account. The concept of the kinematic and dynamic constraint conditions of elastic displacement for flexible parallel robots is used to decouple moving platform's motion equations from those of the sub-chains. The position error and orientation error of moving platform resulted from the links' elastic displacement are calculated. Based on the dynamic model, a method for the inverse dynamic analysis of flexible parallel robots is introduced.

2. Dynamic equations

2.1. Model of flexible beam element

A flexible parallel robot can be divided into several parts which are composed of equal cross-section beam elements. The equal cross-section beam element is usually used to describe a links' elastic displacement. A two-node finite beam element representing a portion of link i of the flexible parallel robots is shown in Fig. 1. The element nodal displacements, or generalized coordinates, are expressed in matrix form as

$$\mathbf{u} = \{u_1, u_2, u_3, u_4, u_5, u_6, u_7, u_8\}^T \quad (1)$$

where u_j , u_{j+4} ($j=1,2,3$ and 4) are axial displacements along the \bar{x} axis, transverse displacements along the \bar{y} axis, and the rotary displacements and curvature displacements with respect to the \bar{z} axis, of nodes 1 and 2, respectively.

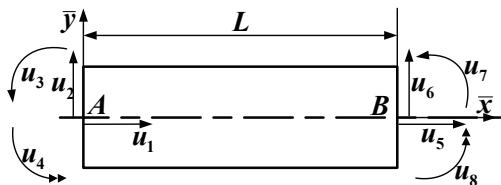


Fig. 1. Model of a flexible beam element

The displacements of a point in the element include axial, transverse, rotary and curvature displacements, expressed as: $S_1(x, t)$, $S_2(x, t)$, $S_3(x, t)$ and

$S_4(x, t)$. These can be described with a set of interpolation functions and generalized coordinates

$$S_i(x, t) = \mathbf{N}_i^T \cdot \mathbf{u} \quad (i = 1, 2) \quad (2)$$

$$S_3(x, t) = (\partial \mathbf{N}_2 / \partial x)^T \cdot \mathbf{u} = \mathbf{N}_3^T \cdot \mathbf{u} \quad (3)$$

$$S_4(x, t) = (\partial^2 \mathbf{N}_2 / \partial x^2)^T \cdot \mathbf{u} = \mathbf{N}_4^T \cdot \mathbf{u} \quad (4)$$

where \mathbf{N}_1 and \mathbf{N}_2 are the vectors of quintic Hermite polynomials and a linear polynomial, respectively.

The elastic motion of a beam element is shown in Fig. 2. Oxy is a global reference frame and $A\bar{x}\bar{y}$ is a local reference frame attached to the left end of link i . So the \bar{x} axis is always directed along the axis of link i in its rigid body configuration (shown in solid lines) which is oriented by angle θ . It is assumed that the deformed position (shown in dashed lines) transforms two nodes, 1 and 2, from their rigid body position A, B and C to their deformed configuration A', B' and C' , respectively.

Now we can derive the dynamic equations of flexible parallel robots by applying the basic beam element developed above.

2.2. Kinetic energy and potential energy of the beam element

The beam element described in Fig. 2 contains a beam with lumped mass attached to both endpoints. The lumped mass physically represents the effect of the actuator mass or payload on the dynamic response. This should not be simply neglected. The total kinetic energy of the element depends on generalized coordinates. Then, considering translating kinetic energy T_{e1} , rotating kinetic energy T_{e2} and the kinetic energy T_{e3} of the lumped mass attached to the endpoints of element, the total kinetic energy T_e of the element can be described as

$$T_e = T_{e1} + T_{e2} + T_{e3} \quad (5)$$

Where

$$T_{e1} = \rho A (v_A^2 L + v_A \dot{\theta} L^2 \sin \theta + \dot{\theta}^2 L^3 / 3) / 2 + \dot{\mathbf{u}}^T \cdot \bar{\mathbf{m}} \cdot \dot{\mathbf{u}} / 2$$

$$+ \dot{\theta}^2 \mathbf{u}^T \cdot \bar{\mathbf{m}} \cdot \mathbf{u} / 2 + \dot{\theta} \dot{\mathbf{u}}^T \cdot \mathbf{b} \cdot \mathbf{u} + \mathbf{u}^T \cdot \mathbf{Y} + \dot{\mathbf{u}}^T \cdot \mathbf{Z}$$

$$T_{e2} = \rho I \dot{\theta}^2 L / 2 + \dot{\mathbf{u}}^T \cdot \mathbf{F} + \dot{\mathbf{u}}^T \cdot \bar{\mathbf{m}}_r \cdot \dot{\mathbf{u}} / 2$$

$$T_{e3} = (m_A + m_B) v_A^2 / 2 + m_B \dot{\theta}^2 L^2 / 2 + m_B \dot{\theta} L v_A \sin \theta + (J_A + J_B) \dot{\theta}^2 / 2 + \dot{\theta}^2 \mathbf{u}^T \cdot \bar{\mathbf{m}}_c \cdot \mathbf{u} / 2 + \dot{\mathbf{u}}^T \cdot \bar{\mathbf{m}}_c \cdot \dot{\mathbf{u}} / 2 + \mathbf{u}^T \cdot \mathbf{Y}_c + \dot{\theta} \dot{\mathbf{u}}^T \cdot \mathbf{b}_c \cdot \mathbf{u} + \dot{\mathbf{u}}^T \cdot \mathbf{Z}_c + \dot{\mathbf{u}}^T \cdot \bar{\mathbf{m}}_j \cdot \dot{\mathbf{u}} / 2 + \dot{\theta} \dot{\mathbf{u}}^T \cdot \mathbf{Z}_j$$

ρ , A and L are density of material, the area of cross-section and the length of the element, respectively. v_A is

the absolute velocity of node A . θ is the angle of \bar{x} axis of the local reference frame with respect to x axis of the global reference frame. I is the moment of inertia of the cross-section with respect to \bar{z} axis passing through the centroid of the element. m_A, m_B, J_A and J_B are lumped mass and lumped rotary inertia at the endpoints of the element, respectively.

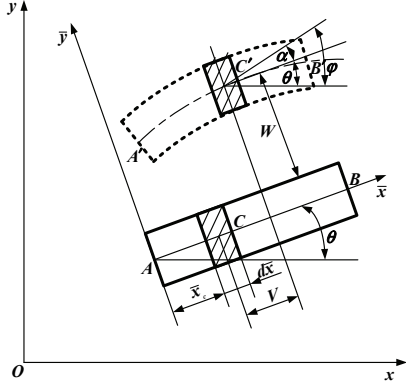


Fig. 2. Elastic motion of a beam element

The total potential energy V_e of the element is composed of the bending-shearing strain energy V_{e1} due to transverse deformations, tensile-compression strain energy V_{e2} due to axial deformations and transverse deformations

$$V_e = V_{e1} + V_{e2} \quad (6)$$

where

$$V_{e1} = EJ_z \mathbf{u}^T \cdot (\boldsymbol{\Omega}_1 + \bar{\mathbf{k}}_1^\lambda + \bar{\mathbf{k}}_2^\lambda + \bar{\mathbf{k}}_3^\lambda) \cdot \mathbf{u} / 2$$

$$V_{e2} = \mathbf{u}^T \cdot (EA\boldsymbol{\chi}_1 + \mathbf{k}_N) \cdot \mathbf{u} / 2$$

where E is tensile modulus of elasticity. J_z is area moment of inertia of the cross-section with respect to z axis.

2.3. Dynamic equations of element

The Lagrangian principle is employed in deriving the motion equations of the element

$$d(\partial T_e / \partial \dot{\mathbf{u}}) / dt - \partial T_e / \partial \mathbf{u} + \partial V_e / \partial \mathbf{u} = \mathbf{Q}_e \quad (7)$$

By substituting equations (5) and (6) into equation (7), and performing the required differentiation and algebraic manipulators, the motion equations of the element can be written in matrix form

$$\mathbf{M}_e \cdot \ddot{\mathbf{u}} + \mathbf{C}_e \cdot \dot{\mathbf{u}} + \mathbf{K}_e \cdot \mathbf{u} = \mathbf{p}_e + \mathbf{f}_e + \mathbf{q}_e \quad (8)$$

where

$$\mathbf{M}_e = \mathbf{m} + \mathbf{m}_c + \mathbf{m}_r + \mathbf{m}_j$$

$$\mathbf{C}_e = 2\dot{\theta}(\mathbf{b} + \mathbf{b}_c)$$

$$\mathbf{K}_e = EJ_z(\boldsymbol{\Omega}_1 + \bar{\mathbf{k}}_1^\lambda + \bar{\mathbf{k}}_2^\lambda + \bar{\mathbf{k}}_3^\lambda) + EA\boldsymbol{\chi}_1 + \mathbf{k}_N$$

$$+ \ddot{\theta}(\mathbf{b} + \mathbf{b}_c) - \dot{\theta}^2(\mathbf{m} + \mathbf{m}_c)$$

$$\mathbf{p}_e = \mathbf{Y} + \mathbf{Y}_c - \dot{\mathbf{Z}} - \dot{\mathbf{Z}}_c - \dot{\mathbf{F}} - \ddot{\theta}\mathbf{Z}_j$$

$\mathbf{M}_e, \mathbf{C}_e$ and \mathbf{K}_e are the mass matrix, damping matrix and stiffness matrix of the element, respectively. Subscript e represents the elemental property. \mathbf{f}_e is the force vector exerted by adjacent elements. \mathbf{q}_e is the external force vector. \mathbf{p}_e is the inertia force vector of the element. Except for \mathbf{f}_e and \mathbf{q}_e , all the terms in equation (8) are given in reference(Zhang, C. et al., 1997).

2.4. Kinematic constraint conditions

AS shown in Fig.3, a parallel robot is composed of a moving platform, namely the end-effector, connected to the base with several independent kinematic chains. Each of these chains contains many independent passive joints and actuated joints.

The relation between the actual configuration (shown as a solid line) and the nominal configuration (shown as a dashed line) can be described using the motion of point P on moving platform, as shown in Fig. 4.

(δ_x, δ_y) and ε are x, y axial displacements and angular displacement of moving platform changing from the nominal configuration to actual configuration, respectively. The local reference frame Pxy is attached to moving platform. The position vector of the endpoint of sub-chain j in actual configuration can be written as

$$\begin{Bmatrix} x'_D \\ y'_D \\ 1 \end{Bmatrix} = \mathbf{R}_{PP} \begin{Bmatrix} x_D \\ y_D \\ 1 \end{Bmatrix} \quad (9)$$

where

$$\mathbf{R}_{PP} = \begin{Bmatrix} 1 & \varepsilon & -\delta_x \\ -\varepsilon & 1 & -\delta_y \\ 0 & 0 & 1 \end{Bmatrix}$$

(x'_D, y'_D) and (x_D, y_D) are position vectors of the endpoint of sub-chain j in actual configuration and

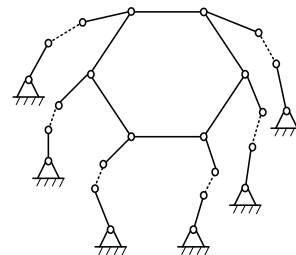


Fig. 3. Abridged general view of parallel robots

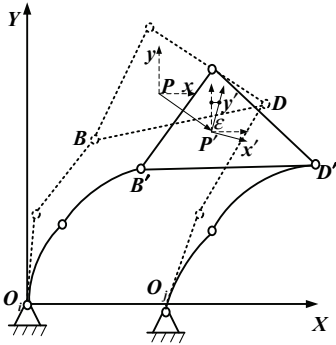


Fig. 4. Relation between the actual configuration and nominal configuration

nominal configuration, respectively. R_{Pp} is the transformation matrix from the global reference frame to the local reference frame $P'x'y'$.

The position vector DD' can be expressed as

$$DD' = \begin{pmatrix} U_{jx} \\ U_{jy} \end{pmatrix} = \begin{pmatrix} x'_D \\ y'_D \end{pmatrix} - \begin{pmatrix} x_D \\ y_D \end{pmatrix} \quad (10)$$

where DD' represents the position vector of the endpoint of the sub-chain j which is changing from the nominal configuration to the actual configuration. U_{jx} and U_{jy} are x, y axial elastic displacements of the endpoint of the sub-chain j , respectively.

By substituting equation (9) and (10) into equation (11), the kinematic constraint conditions of elastic displacements are obtained

$$\begin{Bmatrix} U_{jx} \\ U_{jy} \\ 1 \end{Bmatrix} = \begin{bmatrix} 0 & \varepsilon & -\delta_x \\ -\varepsilon & 0 & -\delta_y \\ 0 & 0 & 1 \end{bmatrix} \begin{Bmatrix} x_D \\ y_D \\ 1 \end{Bmatrix} \quad (11)$$

2.5. Dynamic constraint conditions

The position vector of point P on moving platform can be expressed as

$$\begin{pmatrix} x'_P \\ y'_P \\ \beta' \end{pmatrix} = \begin{pmatrix} x_P \\ y_P \\ \beta \end{pmatrix} + \begin{pmatrix} \delta_x \\ \delta_y \\ \varepsilon \end{pmatrix} \quad (12)$$

where (x'_P, y'_P, β') and (x_P, y_P, β) are the position vectors of point P in the actual configuration and the nominal configuration, respectively.

The dynamic constraint conditions of the flexible planar parallel manipulator are obtained using Newton-Euler formula.

$$\begin{bmatrix} m_P & 0 & 0 \\ 0 & m_P & 0 \\ 0 & 0 & I_P \end{bmatrix} \begin{pmatrix} \ddot{x}'_P \\ \ddot{y}'_P \\ \ddot{\beta}' \end{pmatrix} = \begin{pmatrix} \sum_{j=1}^N f_{jx} \\ \sum_{j=1}^N f_{jy} \\ \sum_{j=1}^N M_j \end{pmatrix} + \begin{pmatrix} \sum F_{ox} \\ \sum F_{oy} \\ \sum M_o \end{pmatrix} \quad (13)$$

where

$$\sum_{j=1}^N M_j = \sum_{j=1}^N \left[(f_{jx}, f_{jy}) \cdot \begin{pmatrix} \sin \phi_j \\ -\cos \phi_j \end{pmatrix} \right] L_j$$

m_P, I_P are mass and rotary inertia of moving platform, respectively. f_{jx}, f_{jy} and M_j are x, y axial internal forces and internal moment exerted on moving platform by sub-chain j , respectively. $\sum F_{ox}, \sum F_{oy}$ and $\sum M_o$ are x, y axial resultant external forces and the resultant external moment exerting on moving platform, respectively. ϕ_j is the inclination angle of x axis of the global reference frame with respect to the vector connecting point P with the endpoint of sub-chain j in the actual configuration. L_j is the distance from point P to the endpoint of sub-chain j . N is the number of sub-chains..

2.6. System dynamic equations

The parallel robot can be conveniently modeled as a system in terms of a set of system generalized coordinates U with respect to the fixed frame Oxy . Therefore a proper transformation between the element and the corresponding system coordinates is essential. This is achieved by applying a linear transformation between the element generalized coordinates u and the corresponding system generalized coordinates U via the appropriate transformation matrix R . Thus

$$u = R \cdot U \quad (14)$$

where

$$R = \begin{bmatrix} \cos \theta & \sin \theta & 0 & 0 & 0 & 0 & 0 & 0 \\ -\sin \theta & \cos \theta & 0 & 0 & 0 & 0 & 0 & 0 \\ 0 & 0 & 1 & 0 & 0 & 0 & 0 & 0 \\ 0 & 0 & 0 & 1 & 0 & 0 & 0 & 0 \\ 0 & 0 & 0 & 0 & \cos \theta & \sin \theta & 0 & 0 \\ 0 & 0 & 0 & 0 & -\sin \theta & \cos \theta & 0 & 0 \\ 0 & 0 & 0 & 0 & 0 & 0 & 1 & 0 \\ 0 & 0 & 0 & 0 & 0 & 0 & 0 & 1 \end{bmatrix}$$

\mathbf{R} represents the transformation matrix from the global reference frame to a local reference frame. This matrix is a function of angle θ . \mathbf{U} is the expression of \mathbf{u} in the global reference frame.

Employing all the motion equations of the basic beam element, the kinematic constraint conditions and dynamic constraint conditions, and expressing in terms of the global coordinates \mathbf{U} , the system dynamic equations are obtained

$$\mathbf{M} \cdot \ddot{\mathbf{U}} + \mathbf{C}' \cdot \dot{\mathbf{U}} + \mathbf{K} \cdot \mathbf{U} = \mathbf{P} + \mathbf{Q} \quad (15)$$

where \mathbf{M} , \mathbf{C}' and \mathbf{K} are the mass, the equivalent damping and the stiffness matrix of system, respectively.

\mathbf{M} , \mathbf{C}' , \mathbf{K} , \mathbf{P} and \mathbf{Q} are the functions of θ , $\dot{\theta}$ and $\ddot{\theta}$.

The damping matrix \mathbf{C}' in equation (15) involves only the equivalent damping of the system. It is generally recognized that the actual damping should contain the structural damping. Therefore, neglecting structural damping in the dynamic model may lead to an unreasonable response. The damping matrix in equation (15) should be modified in order to include structural damping in the model whenever present. Towards this objective, the overall system damping matrix is given as

$$\mathbf{C} = \mathbf{C}' + \mathbf{C}_s \quad (16)$$

Where

$$\mathbf{C}_s = \alpha_1 \mathbf{M} + \alpha_2 \mathbf{K}$$

\mathbf{C} , \mathbf{C}_s represent the total damping and structural damping of the system, respectively. \mathbf{C}_s is derived by using the Rayleigh proportional damping method, and α_1 , α_2 are Rayleigh proportional damping coefficients.

Substituting \mathbf{C}' with \mathbf{C} in equation (15), the general form of the system dynamic equations are obtained

$$\mathbf{M} \cdot \ddot{\mathbf{U}} + \mathbf{C} \cdot \dot{\mathbf{U}} + \mathbf{K} \cdot \mathbf{U} = \mathbf{P} + \mathbf{Q} \quad (17)$$

3. Inverse dynamics analysis

The research on inverse dynamics of the flexible parallel robot is quite difficult. The relation between the position variables, orientation variables and the joint variables can not be determined from the kinematic analysis. These variables must be obtained by solving the dynamic equations. All the generalized coordinates except for the position, orientation, velocity and acceleration of the end-effector remain unknown, and all the system mass matrix, stiffness matrix, damping matrix and generalized forces

are the functions of generalized coordinates. So it is very difficult to solve the inverse dynamic equations.

There are two solutions for inverse dynamics of flexible robots based on the role of the driving forces (moments) in the inverse dynamics equations. Generally, the driving forces are considered as drive force and constrained force, respectively. For the convenience of description, the solutions are called "driving force method" and "driving constraint method" in this paper.

"Driving constraint method" based on the flexible multi-body theory is an accurate method. The driving forces are used as constraints to synthesize the dynamic equations, so the method is widely used for rigid body system. For the flexible body system, the motion differential equation should be integrated to calculate the driving forces even if there is no redundant rigid body freedom. The main drawback of this method is the difficulty in dynamic modeling for multi-link robots. Because the dynamic model of flexible parallel robots based on the flexible multi-body dynamic theory has not been obtained, this method can not be employed in this paper.

The "driving force method" is an approximation method. Firstly, the rigid body motion variables are approximately determined under the assumption that the actual trajectory is carried out by the rigid robot. Such an approximation may lead to definite error in the result. Secondly, the "rigid body driving forces" are derived from the rigid-body motion equations. Thirdly, these "rigid body driving forces" are substituted into the dynamic equations of the flexible robot to calculate the elastic motion variables. Lastly, all these variables are substituted into the equation (18) to calculate the driving forces.

$$\begin{aligned} \sum_{r=1}^k M_{ir} q_r + \sum_{r,s=1}^k \left(\frac{\partial M_{ir}}{\partial q_s} - \frac{1}{2} \cdot \frac{\partial M_{sr}}{\partial q_i} \right) q_s q_r & \quad (i = 1, 2, \dots, k) \\ + \sum_{r=1}^k K_{ir} \cdot q_r + \frac{\partial V}{\partial q_i} & = Q_i \end{aligned} \quad (18)$$

where M_{ir} , M_{sr} and K_{ir} are component of mass matrix and stiffness matrix, respectively. q_s , q_r are the s^{th} and r^{th} generalized coordinate, respectively. V is the system potential energy. Q_i is the i^{th} component of the generalized forces with respect to generalized coordinates. k is the number of generalized coordinates. In order to increase the accuracy of the results, "modified driving force method" is presented here. The object is achieved by performing iterative computations. As we know, the position and orientation vector \mathbf{S} of the end-effector is determined by joint variables θ and elastic deformation of links, thus \mathbf{S} can be expressed as

$$\mathbf{S} = \mathbf{S}(\theta, \mathbf{U}) \quad (19)$$

Joint variables $(\theta, \dot{\theta}, \ddot{\theta})$ and elastic deformation (U, \dot{U}, \ddot{U}) of links are determined by joint driving forces (moments) τ , thus

$$F(\tau) = W \cdot \tau = f(\theta, \dot{\theta}, \ddot{\theta}, U, \dot{U}, \ddot{U}) \quad (20)$$

where W is coefficient matrix.

The simultaneous equations constituted by equation (19) and equation (20) are the universal model of inverse dynamics of flexible robots (Guo, J F., 1992). Due to the complexity of these equations, this model is not suitable for theoretical analysis. Generally, some assumptions are presented to simplify the calculation and obtain the approximate result. In this paper, an iterative computing algorithm is presented to increase the calculating accuracy. Firstly, the trajectory of the end-effector is assumed to be realized by the rigid robot, thus the rigid joint variables θ_i (original value) and "rigid body driving forces (moments)" are calculated and then the elastic deformation U_i is obtained. Secondly, θ_i and U_i are substituted into equation (19) to calculate the position and orientation vector S_i of the end-effector. Because θ_i is derived from the assumption, this will result in the error of the position and orientation vector of the end-effector. The error can be expressed as

$$\Delta S = S_i(\theta_i, U_i) - S_{i-1}^*(\theta_{i-1}^*, U_{i-1}^*) \quad (21)$$

where $S_{i-1}^*(\theta_{i-1}^*, U_{i-1}^*)$ is the position and orientation vector calculated in step $i-1$, and $S_0^*(\theta_0^*, U_0^*) = S(\theta, U)$. If the error is less than the given accuracy ε , θ_i and U_i will be considered as the required values, otherwise let

$$S_i^*(\theta_i^*, U_i^*) = S_{i-1}^*(\theta_{i-1}^*, U_{i-1}^*) - \Delta S \quad (22)$$

Repeat the above-mentioned iterative process until the error ΔS is less than the prescribed accuracy ε . Lastly, the joint variables θ and elastic deformation U are obtained and then the driving forces (moments) are achieved.

4. Numerical simulation and analysis

Because of the complexity of manufacture and control, it is a challengeable task to design and produce a flexible parallel robot, namely all the links are flexible and moving platform is rigid, fulfilled the predefined requirements and adequately revealed the intrinsic characteristics. So far there has been no practicable

flexible parallel robots for the purpose mentioned above. Therefore the numerical example of a flexible planar 3-RRR parallel robot is presented here. Generally, R stands for revolute, therefore RRR represents a kinematic chain composed of, starting from the ground, three rotational joints. With these nomenclature, the actuated joint is underlined. Therefore, a 3-RRR robot is composed of three RRR kinematic chains. A typical 3-RRR planar robot is shown in Fig. 5.

Each link is made of steel with mass density of 7800kg/m³, elastic modulus of 2.1×10¹¹Pa, Poisson's ratio of 0.3. The length of each link is 0.2m, and the cross-section is 0.003m×0.003m. The lumped mass attached to each endpoint of the links is 0.04kg. The length of each edge of the triangular moving platform is 0.042m, and point P is the centroid of moving platform. The mass of moving platform is 0.1kg. The coordinates of the fixed hinge are (-0.3, 0), (0.15, 0.1) and (0.2, 0), respectively.

The motion of point P is described as

$$\begin{cases} X = 0.042 \times \cos(\pi \cdot t/2) \\ Y = 0.25 + 0.042 \times \sin(\pi \cdot t/2) \\ \varphi = 0.01 \times \cos(\pi \cdot t/10) \end{cases} \quad (t = 0 \sim 4s)$$

where X, Y represent x, y axial coordinates of the point P , respectively. φ represents the orientation angle of moving platform. t represents time.

In order to verify the validity of the method, the results are compared with SAMCEF software simulation results. The position errors and orientation errors of point P , shown in Figs. 6-8, are expressed in a global frame. The orientation error can not be calculated by using SAMCEF software, so there is only a numerically calculated result shown in Fig. 8. The results are analyzed as follows. Compared with the results of SAMCEF software simulation, the numerical simulation results show good correspondence and demonstrate the accuracy of the method. The difference between the software simulation results and the numerical simulation results is less than 10%. The dynamic characteristics of flexible parallel robots are illustrated using the model. So the model is useful for dynamic analysis of flexible parallel robots.

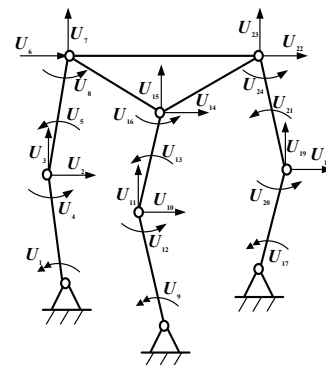


Fig. 5. Generalized coordinates of 3-RRR

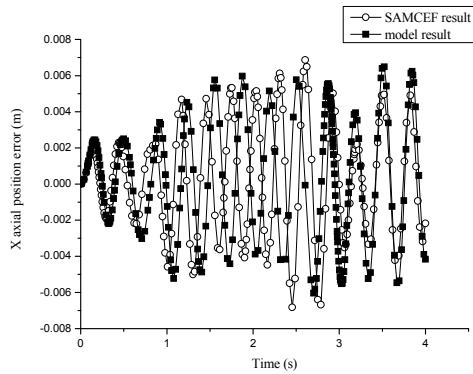


Fig. 6. X axial position error of point P

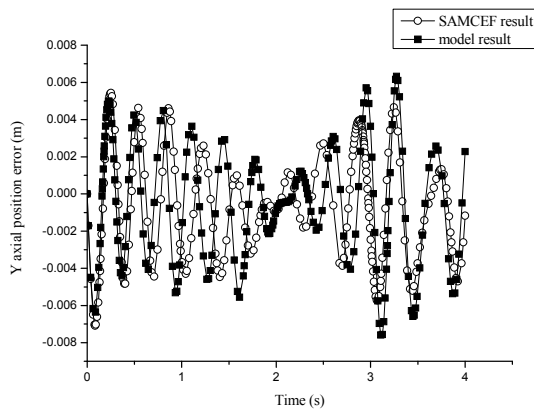


Fig. 7. Y axial position error of point P

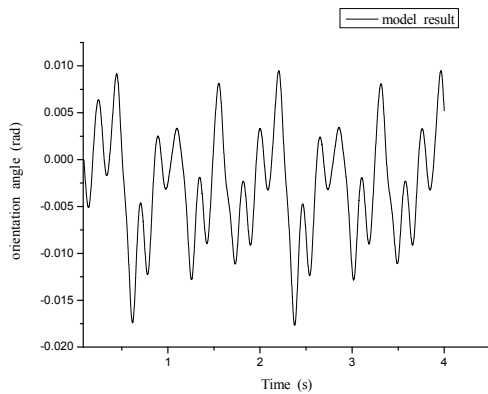


Fig. 8. Orientation error of point P

The maximum position errors and orientation error due to elastic displacement of links are remarkable. The x , y axial position errors are 6mm and 8mm, respectively, and the orientation error is -0.015 rad. Moreover, the position errors of some positions are less, while the orientation error is greater. So it is necessary to analyze both the position errors and orientation error. Orientation error should be taken into account in selecting the working position.

As shown in Figs. 6-8, the frequencies of oscillations of position errors and orientation error are remarkable, and the errors of any position are dramatically different from those of other positions. The results are useful in selecting working positions to fulfill given requirements. Moreover, the actual trajectory oscillates regularly around the nominal trajectory. So the conclusion can be drawn that the actual trajectory is essentially an elastic oscillation.

In order to shorten the paper, only the driving moment of the 1st sub-chain of flexible parallel robot is shown in Fig. 9 (shown in real lines). The driving moment of the rigid one (shown in dashed lines) is also presented.

The driving moment of flexible robot oscillates around the driving moment of rigid robot. The oscillating amplitude is about 0.2Nm. The data and their changing pattern are coincident with the dynamic characteristics of flexible robots. The results verify the validity of the inverse dynamics method presented in this paper.

5. Conclusions

- (1) An approach to dynamic modeling of flexible parallel robots is presented using the kinematic and dynamic constraint conditions of elastic displacements proposed in this paper. It is applicable for dynamic modeling of spatial parallel robots with various kinds of kinematic pairs.
- (2) The links' flexibility and the coupling effects of elastic motion and rigid motion have a significant impact on system performance and stability.
- (3) The dynamic response of flexible parallel robots is drastically different from the response of rigid ones.
- (4) Position errors and orientation error are important performance criteria to measure the capacity of flexible parallel robots. These errors can indicate the motion stability.
- (5) The analysis of the position errors and orientation error is useful to control the vibration of flexible parallel robots.
- (6) The method presented for the inverse dynamic analysis is valid and effective.

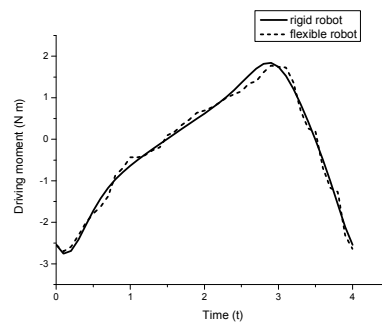


Fig. 9. The driving moment of flexible robot

6. Acknowledgment

This research is supported by National Natural Science foundation of China (50575002), Beijing Natural Science foundation (3062004), Beijing Science and Technology Committee, Beijing Education Committee. The authors also thank Drs. Edmund and Rhoda Perozzi, both of Beijing University of Technology, for assistance in polishing the English.

7. References

- Benosman, M. & Le, V G. (2002). Joint trajectory tracking for planar multi-link flexible manipulator: Simulation and experiment for a two-link flexible manipulator, *Proceedings of International Conference on Robotics and Automation*, IEEE Robotics and Automation society, pp.2461-2466, ISBN: 0-7803-7272-7, Washington, D.C., 2002.5, Institute of Electrical and Electronics Engineers, Washington, USA
- Book, W J. (1990). Modeling, design, and control of flexible manipulator arms: A tutorial review, *Proceedings of the 29th IEEE Conference on Decision and Control*, IEEE Control Systems Society, pp.500-506, ISBN: 90CH2917-3, Honolulu, Hawaii, 1990.12, Institute of Electrical and Electronics Engineers, Hawaii, USA
- Fattah, A. & Misra, A K. & Angeles, J. (1994). Dynamics of a flexible-link planar parallel manipulator in Cartesian space, *Proceedings of the 20th Design Automation Conference*, ASME Design Engineering Division, pp.483-490, ISBN: 0791812839, Minneapolis, Minnesota, USA, 1994.9, American Society of Mechanical Engineers, New York, USA
- Fraid, M. & Lukasiewicz, S A. (2000). Dynamic modeling of spatial manipulators with flexible links and joints, *Computers and Structures*, Vol.75, No.4, 2000.4, pp.419-437, ISSN: 0045-7949
- Gabriel P. (2003). Dynamic finite-element analysis of a planar high-speed, high-precision parallel manipulator with flexible links. *Master thesis*, Graduate department of Mechanical and Industrial Engineering University of Toronto, Toronto, Canada
- Gaultier, P E. & Cleghorn, W L. (1989). Modeling of flexible manipulator dynamics: A literature survey, *Proceedings of the 1st National Applied Mechanism and Robot Conference*, pp.1-10, Cincinnati, Ohio, USA, 1989, American Society of Mechanical Engineers, New York, USA
- Guo, J F. (1992). The method of linearizing dynamic model and solving normal dynamic problems of flexible robots, *Chinese Journal of Mechanical Engineering (English Edition)*, Vol. 5, No.1, 1992.4, pp.53-61, ISSN: 1000-9345
- Lebret, G. & Liu, K. & Lewis, F L. (1993). Dynamic analysis and control of a Stewart platform manipulator, *Journal of Robotic Systems*, Vol. 10, No.5, pp. 629-655, ISSN: 0741-2223
- Jerzy, Z. & Plosa, S W. (2000). Dynamics of systems with changing configuration and with flexible beam-like links, *Mechanism and Machine Theory*, Vol.35, pp.1515-1534, ISSN: 0094-114X
- Lin, J. & Lewis, F L. (1994). A symbolic formulation of dynamic equations for a manipulator with rigid and flexible links. *The International Journal of Robotics Research*, Vol.13, No.5, pp.454-466, ISSN: 0278-3649
- Liu, K. & Lewis, F L. & Lebret, G. et al. (1993). The singularities and dynamics of a Stewart platform manipulator. *Journal of Intelligent and Robotic systems*, Vol.8, No.3, pp. 287-308, ISSN: 0921-0296
- Liu, K. & Lewis, F L. & Fitzgerald, M. (1994). Solution of nonlinear kinematics of a parallel-link constrained Stewart platform manipulator. *Circuits, Systems and Signal Processing*, Vol.13, No.2-3, pp. 167-183, ISSN: 0278-081X
- Santosh, K D. & Peter, E. (2006). Dynamic analysis of flexible manipulators, a literature review. *Mechanism and Machine Theory*, Vol.41, pp.749-777, ISSN: 0094-114X
- Wang, D. & Vidyasagar, M. (1992). Modeling a class of multilink manipulators with the last link flexible. *IEEE Transactions on Robotics and Automation*, Vol. 8, No. 1, pp. 33-41, ISSN: 1042-296X
- Wang, X Y. (2005). Dynamic modeling, experimental identification, and active vibration control design of a "smart parallel manipulator". *Doctor thesis*, Graduate department of Mechanical and Industrial Engineering University of Toronto, Toronto, Canada
- Wang, X Y. & James, K M. (2006). Dynamic modeling of a flexible-link planar parallel platform using a substructuring approach. *Mechanism and Machine Theory*, Vol.41, pp. 671-687, ISSN: 0094-114X
- Yang, J. & Sadler, P. (2000). On issues of elastic-rigid coupling in finite element modeling of high-speed machines, *Mechanism and Machine Theory*, Vol. 35, pp.71-82, ISSN: 0094-114X
- Zhang, C. & Huang, Y Q. & Wang, Z L. et al. (1997). *Analysis and Design of Elastic Linkages*, China Machine Press, ISBN 7-111-05544-6, Beijing, China